A. Brömme, N. Damer, M. Gomez-Barrero, K. Raja, C. Rathgeb,
A. Sequeira, M. Todisco, and A. Uhl (Eds.): BIOSIG 2022,
Lecture Notes in Informatics (LNI), Gesellschaft für Informatik, Bonn 2022

Fingers Crossed: An Analysis of Cross-Device Finger Vein Recognition

Tuğçe Arıcan,[1] Raymond Veldhuis,[2] Luuk Spreeuwers,[3]

Abstract: Finger veins are one of the emerging biometric traits attracting many researchers in biometric recognition. Despite the growing literature on finger vein recognition, little interest has been shown in the impact of acquisition devices on recognition performance due to the lack of a multi-sensor finger vein database. This work aims to fill this gap by creating such a database using five different acquisition devices. We then analyze their impact on finger vein recognition performance. The analysis shows two main challenges that decrease recognition performance, namely scaling between device sensors and horizontal shifts between image pairs. The findings of this research give insight into developing more robust finger vein recognition algorithms.

Keywords: Finger vein recognition, cross-sensor comparison, vein pattern comparison.

1 Introduction

Finger vein recognition (FVR) is performed by comparing random vein structures beneath the skin. Since they are not visible to the eye, they do not leave any traces and stealing vein patterns is more difficult compared to other biometrics like face or finger prints. Maximum Curvature [MNM07], Repeated Line Tracking [MNM04], and Principal Curvatures [Ch09] methods are commonly used for finger vein extraction which are then compared for recognition. These methods are considered robust against illumination and generally provide a baseline for comparison with other methods. Deep learning models [Ta19, SKP19] achieved the state-of-the-art results on some publicly available finger vein datasets.

Despite the considerable amount of research on finger vein extraction and recognition, there is only a little work exploring the impact of different acquisition devices. Existing research on interoperable FVR either analyze the impact of the sensor on preprocessing steps on existing finger vein datasets [Ya15], or perform cross-sensor recognition on sensors having very similar designs [KPU18].

This work analyses the effect of acquisition devices on FVR with a cross-sensor dataset captured by five different acquisition devices. This research aims to expose the challenges on cross-sensor FVR, which could lead to developing more robust FVR algorithms.

[1] University of Twente, EEMCS-DMB, Enschede, The Netherlands, t.arican@utwente.nl
[2] University of Twente, EEMCS-DMB, Enschede, The Netherlands, r.n.j.veldhuis@utwente.nl
[3] University of Twente, EEMCS-DMB, Enschede, The Netherlands, l.j.spreeuwers@utwente.nl

2 Related Work

Vein extraction is one of the most common ways to perform FVR. Miura et.al. [MNM07] used curvatures of finger vein image profiles to extract vein patterns. Together with a matching method, based on correlation of binary vein patterns, the authors achieved an impressive recognition rate on a private dataset. The Maximum Curvature method is one of the most well performing vein extraction approaches in literature.

There are a few studies analyzing the effect of the acquisition device on FVR. Yang et.al. [Ya15] showed that the device characteristics affect the accuracy of extracted Region of Interest (ROI). Though the proposed method was able to extract ROIs accurately on different finger vein datasets, the data had a relatively simple background. Its performance on images with more complex backgrounds is still unclear. Kauba et.al. [KPU18] achieved 0.28% Equal Error Rate (EER) on a cross-sensor dataset collected from 2 sensors they developed. Despite the impressive recognition performance, the sensors used in this work have almost the same design except for the illumination modules. In this regard, this work gives a limited insight about sensor interoperability.

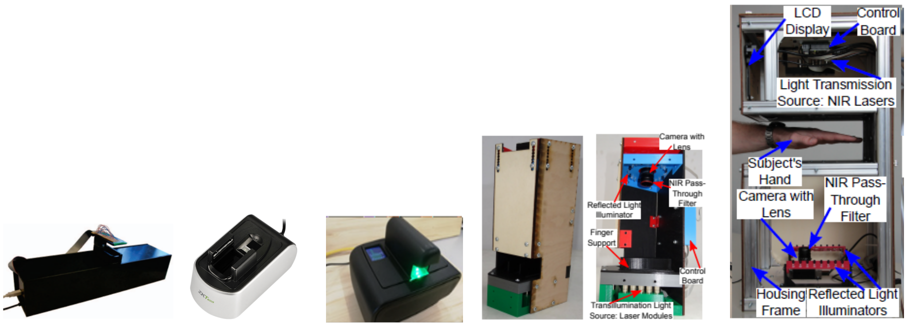

(a) UTFV (b) ZKTeco (c) IDIAP (d) PLUSVLaser (e) PLUSVContactless

Fig. 1: Finger vein sensors used in data acquisition.

3 Methodology

Finger Vein Acquisition: Finger vein acquisition is performed under Near-Infrared (NIR) radiation since hemoglobin in blood cells mostly absorbs the radiation while soft tissues mostly scatter it. This generates a pattern of shadows on a finger vein image [No22]. Light transmission mode, where the camera captures NIR radiations passing through the finger, is the most researched method in literature [YYL09, KZ11, TV13, KPU18, KPU19].

Maximum Curvature: The Maximum Curvature method proposed by Miura et al. [MNM07] uses curvatures of finger vein image profiles where the local maxima of a curvature represents a vein point. Later these maxima locations are connected to obtain a complete vein pattern. This method does not consider the width of the vein, therefore the extracted vein pattern has the same width everywhere. As a final step, extracted veins are binarized by comparing against the median value of the vein patterns. The Maximum Curvature method is one of the most well performing finger vein extraction methods in literature.

Miura Match: The matching method proposed by Miura et.al. [MNM07] is based on finding the maximum correlation between a pair of binary finger vein patterns. In this method, a window is cropped from a reference vein pattern and is correlated with a probe vein pattern. The maximum correlation is considered as the match score of an image pair. The size of the window is a hyper parameter. Miura match is capable of compensating small shifts between finger vein images.

Maximum Curvature and Miura match are relatively old approaches in FVR. Nowadays, deep learning approaches replace these methods and achieve state-of-the-art recognition performance on publicly available finger vein datasets[Ta19, SKP19]. Yet, deep learning methods are black box approaches where their internal logic and extracted features are not easily interpretable. On the other hand, Maximum Curvature provides visual features which allow us to investigate the differences among vein patterns captured by several acquisition devices in this work. Miura match shows how finger vein comparison is performed among different acquisition devices. Therefore, in order to have a deeper understanding of how different acquisition devices affect finger vein recognition, Maximum Curvature and Miura match are chosen as feature extraction and feature comparison methods in this work.

4 Data Acquisition and Datasets

A cross-sensor finger vein database has been created as a collaboration of the University of Twente, Salzburg University, and the IDIAP research institute. Finger vein images of 59 participants were initially collected using five different sensors. Prior to acquisition, participants were informed about the process and asked to fill and sign a consent form. Age, gender, and ethnicity were collected as metadata. Each participant has been given a unique identifier number for anonymization purposes. After filling and signing the consent form, each participant was instructed to go through each of the five sensors and donate their finger vein images. For each participant, three fingers, namely index, middle, and ring fingers of both hands were captured in two sessions. Because of acquisition quality issues and less participants showing up for the second session, the amount of data collected per device varies. The acquired data is available on request. Table 1 presents information about the devices, and some samples from each sensor can be found on Figure 2.

Sensor Name	# Subjects session #1 / #2	Images	Resolution	Illumination Type	Illumination Side
UTFV [TV13]	58 / 45	618	340 x 648	LED	Top
ZKTeco [ZK]	58 / 46	624	240 x 320	LED	Two-Side
IDIAP [ID]	55 / 41	576	320 x 240	LED	Top
PLUSVLaser [KPU18]	43 / 7	294	427 x 611	Laser	Bottom
PLUSVContactless [KPU19]	49 / 7	342	180 x 499	Laser	Top

Tab. 1: Summary of the acquisition devices.

UTFV: UTFV (Fig. 1a) was developed by the University of Twente[TV13] and has a half open design to help users with finger placement, restricting finger movements.

ZKTeco: ZKTeco [ZK] (Fig. 1b) captures both finger prints and veins at the same time. During data acquisition, only the finger vein sensor was activated.

IDIAP: This sensor was developed by the IDIAP research institute in collaboration with GlobalID (Fig. 1c). It captures left, right and center views of a finger. Only the center image is used in this research. The device has a closed design and it is not equipped with a finger support. Due to the high degree-of-freedom of this sensor, images are generally captured with distortions like rotations or finger bendings. Moreover, the device frame interferes the background of the image, which requires more preprocessing effort.

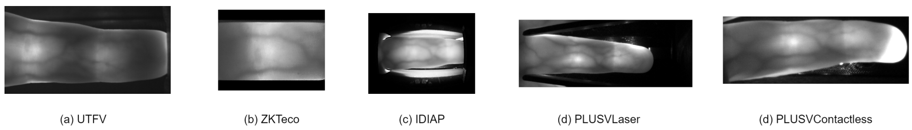

Fig. 2: Finger vein images from different sensors.

PLUSVLaser: PLUSVLaser (Fig. 1d) was developed by Salzburg University [KPU18] and captures both dorsal and palmar images in both transmission and reflection modes. During data acquisition, palmar side images are captured in transmission mode. The device captures 3 fingers at a time, and is equipped with a finger support guiding the user's hand placement. This device does not follow the naming protocol instructed during data acquisition, therefore the link between the subjects of this device and the other device is lost. Moreover, only 7 out of 43 subjects had a second session.

PLUSVContactless: PLUSVContactless (Fig. 1e) also was developed by Salzburg University [KPU19] and captures both hand and finger vein images. During data acquisition, only finger vein images were captured. This device is fully contactless and does not provide any support for fingers. Yet, it is equipped with a touchscreen which shows a live stream from the camera to inform the user of their finger locations. Similar to PLUSVLaser, the naming protocol was not followed for this device, and 7 out of 49 subjects had two sessions

5 Experiments

Only UTFV and ZKTeco data is used in cross-sensor verification experiments, since the data from these sensors are complete. IDIAP data is not utilized for verification experiments due to time limitations and high preprocessing requirements for this device. The remaining 2 devices, together with IDIAP, are utilized to explore the impact of the acquisition device on finger vein extraction and comparison.

Evaluation Protocol: Performance on UTFV and ZKTeco sensors is assessed by using Equal Error Rate (EER), Receiver Operating Characteristics (ROC) curves, and False Non-Match Rate(FNMR) at where False Match Rate(FMR) equals to 0.1%. For genuine scores, all possible genuine matches are considered. For imposter scores however, for each reference image one probe image is selected from all other finger images. Therefore, the number of genuine and imposter comparisons are equal. The UTFV dataset involves 1080 comparisons in total, while number of total comparisons is 1104 for ZKTeco data. In a cross-sensor setting, 2160 image pairs are generated in total.

Cross-sensor matching performance of the rest of the sensors is evaluated by comparing match similarity histograms of each sensor pair. Single-sensor cases consist of 168 genuine and 168 imposter image pairs, while in cross-sensor cases, 336 genuine and 336 imposter image pair comparisons are performed.

	UTFV (Probe)	ZKTeco (Probe)
UTFV (Reference)	1.7	89.7
ZKTeco (Reference)	89.7	22.4

Tab. 2: Performance comparison on UTFV, ZKTeco, and cross-sensor case in FNMR@FMR=0.1% in percentage.

Single and Cross-Sensor Finger Vein Verification: Verification experiments are performed by using the Maximum Curvature and Miura match methods, which are one of the well performing finger vein methods in literature. Before vein extraction, images are passed through a preprocessing pipeline which includes contrast enhancement (CLAHE)[Zu94], edge detection [LLP09] and rotation correction [Hu10]. In this cross-sensor case, the probe image is scaled to the reference device sensor resolution using bicubic scaling. Before the comparison, the probe image is aligned with the reference image.

	UTFV (Probe)	ZKTeco (Probe)
UTFV (Reference)	0.57	26.75
ZKTeco (Reference)	26.14	7.4

Tab. 3: Performance comparison on UTFV, ZKTeco, and cross-sensor case in EER(%).

Table 3 compares verification performances on single and cross-sensor cases. 0.57% EER achieved by UTFV is in line with the verification performance indicated in [TV13]. While ZKTeco performs significantly worse compared to UTFV by achieving 7.4% EER on the same fingers. When ZkTeco is the reference device, UTFV achieves 26.14% EER, and 89.7% FNMR@FMR=0.1%(Tab. 2), which indicates a significant performance drop compared to the case where UTFV is the reference device.

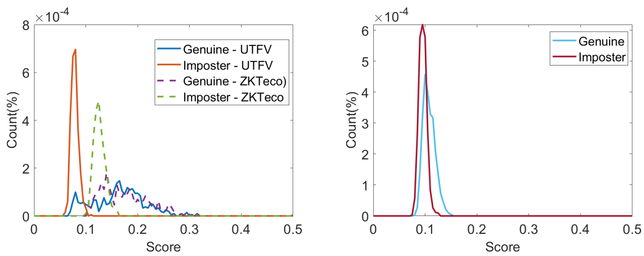

(a) Single sensor setting
(b) Cross-sensor setting

Fig. 3: Similarity histograms of (a) single sensor and (b) cross sensor cases

The ROC curve(Fig. 4a) and FNMR-FMR plots(Fig. 4b) also present the drastic change in verification performance in the cross-device setting. Figures 3a and 3b indicate that in the cross-sensor case, genuine match scores substantially decrease, and their histograms become almost indistinguishable from imposter histograms.

Cross-sensor Finger Vein Comparison: Further analyses of the impact of the acquisition device is performed on 7 subjects from all sensors. In addition to preprocessing, a scaling factor is calculated to match the reference device sensor resolution.

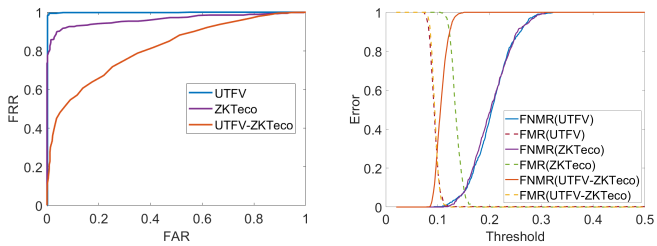

(a) ROC comparison (b) FNMR - FMR comparison

Fig. 4: Performance (a) ROC plots, (b) FNMR - FMR plots.

With the change of the reference device, match scores significantly deviate from the single-device case. Almost all genuine histograms resemble an imposter histogram (Fig. 5, Fig.6, Fig. 7). Due to page limitations, only two comparisons per probe sensor are presented here.

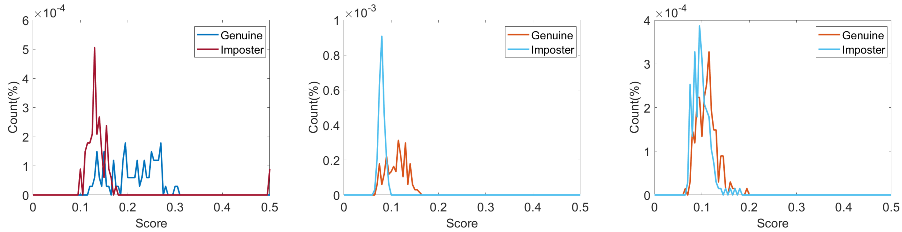

(a) IDIAP (b) UTFV (c) PLUSVLaser

Fig. 5: Cross-sensor match scores where where IDIAP sensor is the probe.

Among all cross-device pairs, when UTFV is chosen as the reference device (Fig. 5b, Fig. 7b), the match score histogram resembles single-device case, despite the significant decrease in genuine match scores. Especially when IDIAP is the probe sensor, separation between genuine and imposter pairs is more prominent (Fig. 5b).

On the other hand, when UTFV is paired with PLUSVLaser, the match score histogram is not similar to the single-device case anymore. With this setting, only a few genuine pairs are able to be distinguished from the imposter pairs (Fig. 6b).

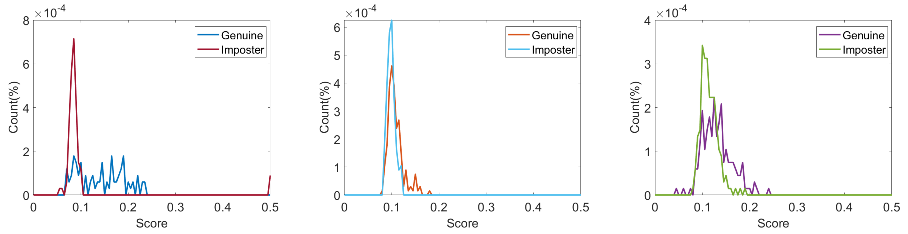

(a) PLUS_FV_Laser (b) UTFV (c) PLUSVContactless

Fig. 6: Cross-sensor match scores where PLUSVLaser is the probe.

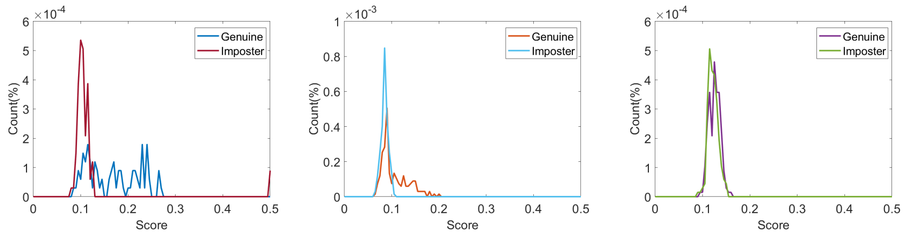

(a) PLUSVContactless (b) UTFV (c) ZKTeco

Fig. 7: Cross-sensor match scores where PLUSVContactless is the probe.

6 Discussion

Verification performance of UTFV data (0.57% EER and 1.7% FNMR@FMR=0.1%) is in line with the results presented in [TV13] (0.4% EER). Participants were given little instruction about their finger placement during cross-sensor data collection. Similar results achieved under a relatively uncontrolled setting implies that UTFV is able to capture high quality vein images under challenging conditions.

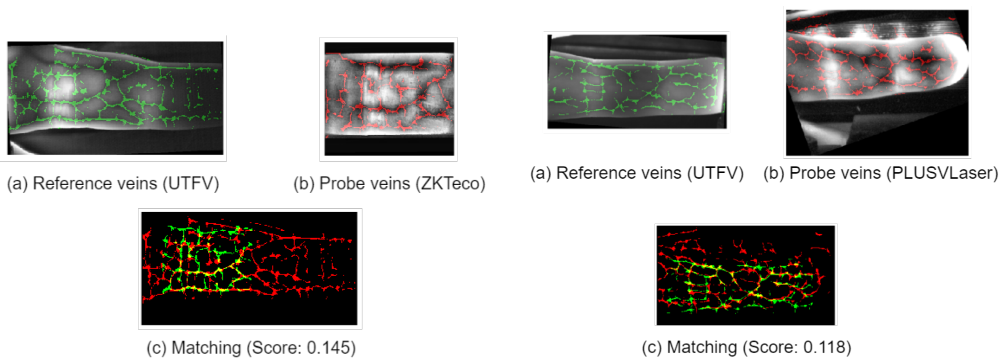

(a) UTFV - ZKTeco genuine pair (b) Missing veins on UTFV-Laser pair

Fig. 8: Sample cross-device matches

When UTFV images are paired with ZKTeco images, even though it is possible to find reasonably good genuine matches between these devices(Fig. 8a), match scores are significantly low due to poor acquisition and illumination quality of ZKTeco.

Challenges observed in cross-sensors pairs mostly stem from differences in device properties. An improper scaling factor is one of the reasons for low genuine match scores when devices, having a high degree-of-freedom like IDIAP and PLUSVContactless, are paired together. On the other hand, when UTFV is the reference device, scaling is less of an issue. This device does not give much freedom to the user about finger placement by design.

Illumination type differences between devices could affect the captured vein patterns. Especially devices equipped with Laser-NIR modules capture veins on phalanges more clearly compared to devices having LED-NIR modules. When a finger is not properly illuminated by LEDs, veins on phalanges are not well extracted. Therefore, matching generates a lower score even if the correct match is found between image pairs(Fig: 8b).

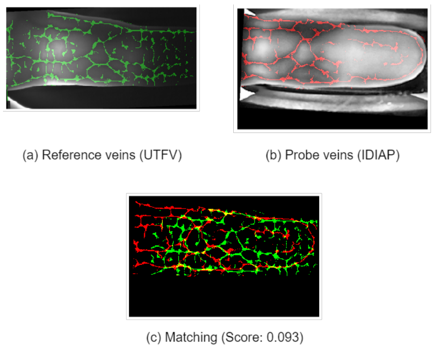

(a) Extreme shift on UTFV-IDIAP sensor

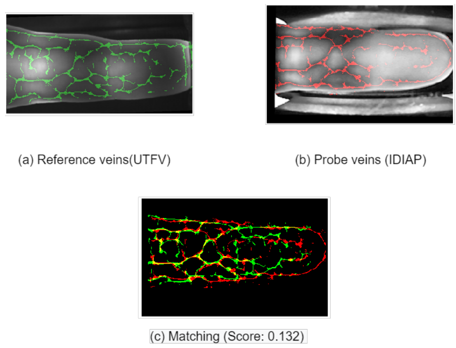

(b) UTFV-IDIAP pair

Fig. 9: UTFV-IDIAP pairs

Differences in device properties causes horizontal shifts between cross-sensor image pairs. Finger roots captured by PLUSVLaser spontaneously introduces a shift on UTFV data. Also, due to lack of finger support, IDIAP images exhibit extreme movements on the horizontal axis(Fig. 9a). These shifts are one of the main reasons of low match scores of genuine pairs, yet they can be rather easily corrected by implementing an additional horizontal alignment step before comparisons.

Despite all the differences among the acquisition devices presented here, it is still possible to find proper cross-device genuine matches. Figure 9b and Figure 10 shows some of these good genuine matches in several cross-device settings. Yet, the match scores are low compared to single-device case due to the challenges mentioned above.

7 Conclusion and Future Work

This work analyses cross-sensor finger vein recognition on data collected by five different acquisition devices from two universities and a research institute. Despite the difficulties faced in data gathering, the results give some insight about challenges on cross-sensor finger vein recognition, also imply that interoperable finger vein recognition is possible.

We found two main challenges to cross-device finger vein recognition. The first is finding a proper scaling factor for scaling the probe image resolution to match that of the reference device. Due to the high degree-of-freedom introduced by different devices, it is challenging to find a fixed scaling factor in many cases.

The second challenge is the horizontal shift between images that is introduced due to device characteristics. The used matching algorithm cannot compensate for this adequately. Moreover, other deformations, such as finger rotations, bendings, etc., complicate cross-device image comparisons. However, shifts can relatively easily be solved by an additional horizontal alignment step, and the rotations can be compensated for by using multi-view finger vein imaging.

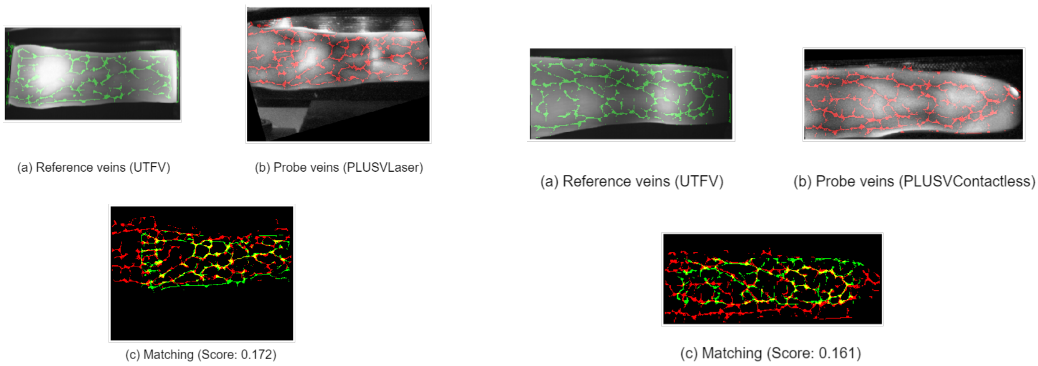

(a) UTFV-PLUSVLaser pair

(b) UTFV-PLUSVContactless pair

Fig. 10: High match score genuine pairs

Cross-device finger vein verification brings multiple challenges to tackle. Yet, some of the image comparisons clearly indicate that it is possible to find relatively good matches between different device images. These findings give valuable insight and open up ways for developing more robust finger vein recognition algorithms.

References

[Ch09] Choi, J. H.; Song, W.; Kim, T.; Lee, S.; Kim, H. C.: Finger vein extraction using gradient normalization and principal curvature. In: Image Process.: Mach. Vis. Appl. II. volume 7251. SPIE, pp. 359–367, 2009.

[Hu10] Huang, B.; Dai, Y.; Li, R.; Tang, D.; Li, W.: Finger-vein authentication based on wide line detector and pattern normalization. In: Int. Conf. Pattern Recognit. IEEE, pp. 1269–1272, 2010.

[ID] IDIAP finger vein sensor.

[KPU18] Kauba, C.; Prommegger, B.; Uhl, A.: Focussing the beam-a new laser illumination based data set providing insights to finger-vein recognition. In: BTAS'18. IEEE, pp. 1–9, 2018.

[KPU19] Kauba, C.; Prommegger, B.; Uhl, A.: Combined fully contactless finger and hand vein capturing device with a corresponding dataset. Sensors, 19(22):5014, 2019.

[KZ11] Kumar, A.; Zhou, Y.: Human identification using finger images. IEEE Trans. on Image Process., 21(4):2228–2244, 2011.

[LLP09] Lee, E. C.; Lee, H. C.; Park, K. R.: Finger vein recognition using minutia-based alignment and local binary pattern-based feature extraction. Int. J. Imaging. Syst. Technol., 19(3):179–186, 2009.

[MNM04] Miura, N.; Nagasaka, A.; Miyatake, T.: Feature extraction of finger-vein patterns based on repeated line tracking and its application to personal identification. Machine vision and applications, 15(4):194–203, 2004.

[MNM07] Miura, N.; Nagasaka, A.; Miyatake, T.: Extraction of finger-vein patterns using maximum curvature points in image profiles. IEICE Trans. Inf. Syst., 90(8):1185–1194, 2007.

[No22] Normakristagaluh, P.; Laanstra, G. J.; Spreeuwers, L.; Veldhuis, R.: Understanding and modeling finger vascular pattern imaging. IET Image Process., 16(5):1280–1292, 2022.

[SKP19] Song, J. M.; Kim, W.; Park, K. R.: Finger-vein recognition based on deep DenseNet using composite image. IEEE Access, 7:66845–66863, 2019.

[Ta19] Tang, S.; Zhou, S.; Kang, W.; Wu, Q.; Deng, F.: Finger vein verification using a Siamese CNN. IET Biometrics, 8(5):306–315, 2019.

[TV13] Ton, B. T.; Veldhuis, R. NJ: A high quality finger vascular pattern dataset collected using a custom designed capturing device. In: ICB'13. IEEE, pp. 1–5, 2013.

[Ya15] Yang, L.; Yang, G.; Zhou, L.n; Yin, Y.: Superpixel based finger vein ROI extraction with sensor interoperability. In: ICB'15. IEEE, pp. 444–451, 2015.

[YYL09] Yang, W.; Yu, X.; Liao, Q.: Personal authentication using finger vein pattern and finger-dorsa texture fusion. In: Proc. ACM Int. Conf. Multimedia. pp. 905–908, 2009.

[ZK] ZKTeco FVP10R fingerprint and finger vein combined sensor.

[Zu94] Zuiderveld, K.: Contrast limited adaptive histogram equalization. Graphics gems, pp. 474–485, 1994.